

## PHOTOGRAMMETRIC WOUND MEASUREMENT WITH A THREE-CAMERA VISION SYSTEM

Saskia M. Boersma\*, Frank A. van den Heuvel\*, Adam F. Cohen\*\*, Rick E.M. Scholtens\*\*\*

\*Department of Geodetic Engineering

Delft University of Technology, Delft, The Netherlands

\*\*Centre for Human Drug Research, Leiden, The Netherlands,

\*\*\*Het Groene Hart Ziekenhuis, Gouda, The Netherlands

[Saskia\\_Boersma@hotmail.com](mailto:Saskia_Boersma@hotmail.com), [F.A.vandenHeuvel@geo.tudelft.nl](mailto:F.A.vandenHeuvel@geo.tudelft.nl), [ac@chdr.nl](mailto:ac@chdr.nl)

Working Group V/4

**KEY WORDS:** Accuracy, calibration, Digital Surface Model, medical, wound measurement, trinocular vision system

### ABSTRACT

A three-camera vision system is developed for the measurement of the shape and volume of wounds, especially pressure sores. This system is able to assist physicians in monitoring the healing process of these wounds. The vision system consists of three progressive scan video cameras that are mounted on a triangular frame with a light source with optional texture projection in the centre. The cameras are not designed for high accuracy measurement purposes. This makes the calibration of the system decisive for the accuracy of the Digital Surface Model (DSM). Eight image triplets of a testfield are acquired for system calibration. A least squares bundle adjustment determines the camera calibration parameters as well as the exterior orientation parameters of the cameras in the frame. A commercial software package, designed for aerial photogrammetry, automatically generates a DSM. A DSM is computed for each of the three image pairs. Differences between the three models are calculated to get insight in the obtained precision of the DSM. To increase the quality of the DSM, the three models are combined to form one final DSM. The resulting DSM is used to calculate the wound features of interest. The applicability of the technique in practice is tested on artificial and real wounds. The comparison between different models showed that a precision of better than 0.7 mm in height could be achieved in the DSM generation using texture projection. Future work has to concentrate on the integration of the components in one user-friendly real-time measurement system for wounds, and on further improvement of the accuracy of the system.

## 1 INTRODUCTION

### 1.1 Motivation

A recent nation-wide prevalence survey in The Netherlands revealed the prevalence of pressure sores to be 14 percent among patients in university hospitals, 20 percent in general hospitals, 29 percent in residents of nursing homes and 12 percent in residential care homes. The annual direct costs of pressure sores in The Netherlands are estimated to be at least 0.5 billion Euro (Health council of The Netherlands, 1999). The medical profession is seeking methods address this problem. In order to investigate methods for curing pressure sores a physician has to be able to judge the healing process. The interpretation of the results is subjective, because there is a great variation in the measurements of wound healing. Consequently, it is difficult to analyse research results. Therefore, there is a need for an objective and practical method to determine the shape of these wounds and derived quantities, such as the contour and the volume.

### 1.2 Pressure sores

Pressure sores, also known as pressure ulcers or bed sores, are damages of the skin caused by prolonged pressure on an area of the body having a bony prominence with a relative thin protective covering, such as the buttocks and heels. Whether pressure sores start to develop depends on patient related factors. The most important of these factors are age, neurological condition, dietary status, blood circulation and how moist the skin is (Health council of The Netherlands, 1999). Four stages are distinguished in the development of pressure sores. Stage 1 is a redness that does not disappear on pressure. In stage 2 a blister develops above the red area and often the blister opens. Stage 3 is a superficial decubitus that is limited to the upper skin. Finally in stage 4 there is exposure of underlying tissue, such as muscle or bone. Figure 1 shows examples of pressure sores in the four different stages.

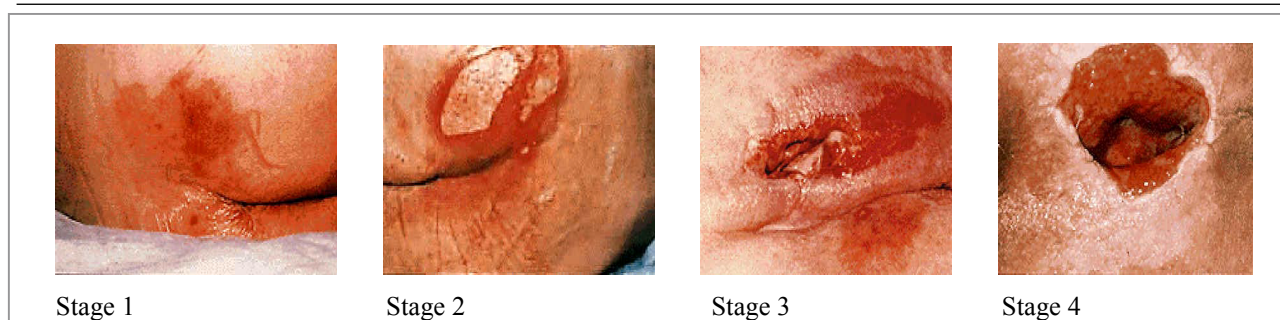


Figure 1: Different stages of pressure sores (Van Dijk, 2000)

### 1.3 Objective

This research focuses on the possibilities to measure the metrical features of pressure sores using a three-camera vision system. The central question in this research is

*Which accuracy can be achieved in the measurement of the metrical features of pressure sores with a three-camera vision system?*

The metrical features that have to be determined in order to compare different curing methods in an objective way are the volume and eventually related quantities such as the contour and surface of the wounds.

### 1.4 Related research

Traditional methods to measure pressure sores are based on determination of the volume by instilling fluid materials into the ulcer. Such methods have many disadvantages such as pain, irritation, allergic reaction, and inexactness. Single photographs only provide a limited amount of information concerning the volume and therefore do not reveal the beginning of a healing process in the bottom of an ulcer (Eriksson, 1979). Single photographs or video images are also used to measure wounds (Ring, 1985). These techniques are unable to supply 3D information and are limited to relatively small surfaces. Ng *et al* (1994) used laser to measure wounds, based on measurement of the distance of the laser array. Plassman *et al* (1995) developed a method to measure the volume of wounds with structured light. Stereophotogrammetry may also provide 3D information. Bulstrode *et al* (1986) and Eriksson *et al* (1979 and 1984) use analogue stereophotogrammetry to determine the volume of wounds. The disadvantage of this method is the large instruments. Furthermore, photographs need to be developed before further processing and thus real-time results are not possible. De Jong (1996) proved that digital stereophotogrammetry is a good method to acquire 3D information on wounds. She used only one camera and thus the two images of the stereopair were not made simultaneously. The approach resulted in a limited precision.

## 2 SYSTEM CONFIGURATION

The configuration of the vision system was designed taking into account the type of camera, the objects to be measured, the illumination, the targets, the flexibility, and the costs of the system.

### 2.1 Premises

For this research we used three Sony XC-55 progressive scan video cameras. The cameras are connected to a frame grabber in a personal computer. This gives the possibility to view the three images during image acquisition. The focal length of the lens of the cameras is approximately 6 mm. The image size is 640 x 480 pixels, with a pixel size of 7.4 x 7.4  $\mu\text{m}$ .

The objects to be measured are pressure sores at different parts of the body. The images should cover the wounds completely, together with a part of the surrounding healthy skin, because the volume of the wound will be determined using interpolation from this surrounding healthy skin.

The quality of the illumination is important for the accuracy of the measured points. The illumination should be uniform and illuminate the object as equal as possible. Since wounds have a moist surface, specular reflections should be avoided as much as possible. It is not necessary to use a very strong illumination, because the cameras are very sensitive to light. However, there should be sufficient light to allow a good depth of field. In case of lack of texture of the human skin, additional texture projection has to be used. Lack of texture causes difficulties in the matching process during DSM generation.

Furthermore, no reference information is required during image acquisition. No reference frame or scale bar is required when the wound images are made. The cameras are mounted, with a fixed position, in a triangular frame. The calibration process determines the position of the cameras in the frame. The software for the DSM generation uses this information as exterior orientation data.

The system should be as flexible as possible for the use in a hospital environment. This implies that it should be as light and small as possible. Taking into account the requirements described above, we designed the following vision system.

## 1.2 Final design

The three progressive scan video cameras are mounted on a triangular frame with a light source and texture projection in the centre (Figure 2). The distance between the cameras is fixed to 15 cm. The base-to-height ratio of 1:2 implies that the distance from the cameras to the wounds has to be approximately 30 cm. The cameras are mounted in a slightly convergent way.

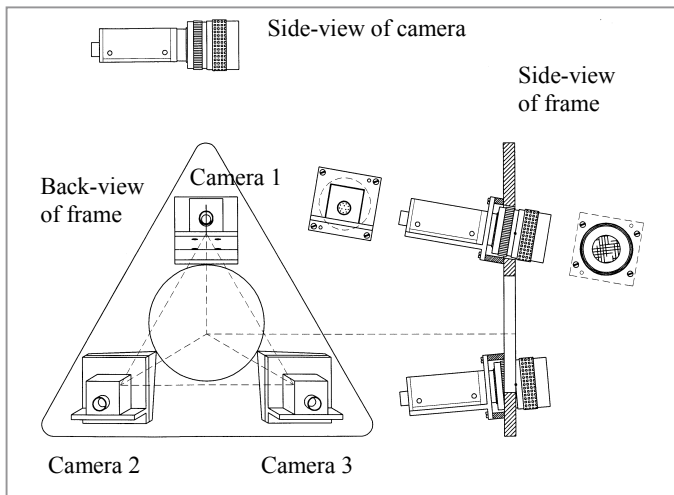


Figure 2: Camera configuration in frame (illumination through the hole in the center)



Figure 3: Picture of system configuration

## 3 CALIBRATION

### 3.1 Purpose of calibration

The cameras we used are non-metric and not designed for high accuracy purposes. This makes the calibration of the system decisive for the accuracy of the DSM. The calibration consists of two different parts: the calibration of the interior orientation including lens distortions of the individual cameras and the calibration of the frame in which the exterior orientation elements of the three cameras are determined.

A complete camera calibration includes radiometric aspects (e.g. the compensation of different sensitivity of CCD sensor cells) as well as geometric aspects. No radiometric camera calibration is performed. The geometric camera calibration involves the determination of the focal length, the location of the principal point and the parameters of the lens distortion. The software package Bingo (Kruck, 1998) is used. This package enables us to determine calibration parameters for more than one camera simultaneously.

### 3.2 Calibration set-up and measurement

We calibrated the system using a testfield of 30 x 40 cm with 63 targets in a regular grid with a mutual distance of 9 cm. Six targets were placed 8 cm above the plane to establish a 3D configuration of the targets. The circular targets are black on a white background with a diameter of 0.5 cm (Figure 4). A total of 8 image triplets (figure 5) were made, 4 convergent and 4 normal case scenes according to Wester-Ebbinghaus (1983). This results in a total of 24 images. Every target was imaged in average in 18 images. We applied template matching for subpixel image measurement. The co-ordinates of the image points were measured with template matching with an average precision of  $3 \times 10^{-4}$  mm, corresponding to an precision of 5 % of a pixel.

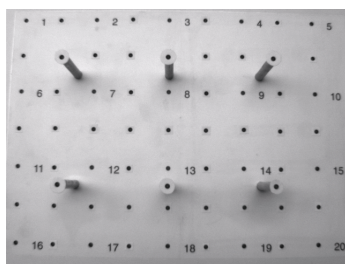


Figure 4: Testfield

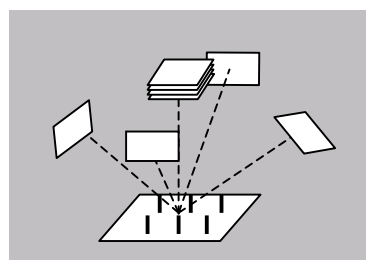


Figure 5: Configuration of 8 images

### 3.3 Bundle adjustment

The parameters of the interior orientation of the three cameras and the exterior orientation for each camera were determined with a least squares bundle adjustment. A set of 5 additional parameters was used to compensate systematic errors (figure 6). Non-significant and non-determinable parameters were excluded from the estimation process in an automatic way (Kruck, 1998). The average standard deviation of the 3D co-ordinates is 0.1 mm in X and Y, and 0.2 mm in Z. A root mean square of image co-ordinate residuals of 5 % of a pixel was achieved, corresponding to 37 microns in object space.

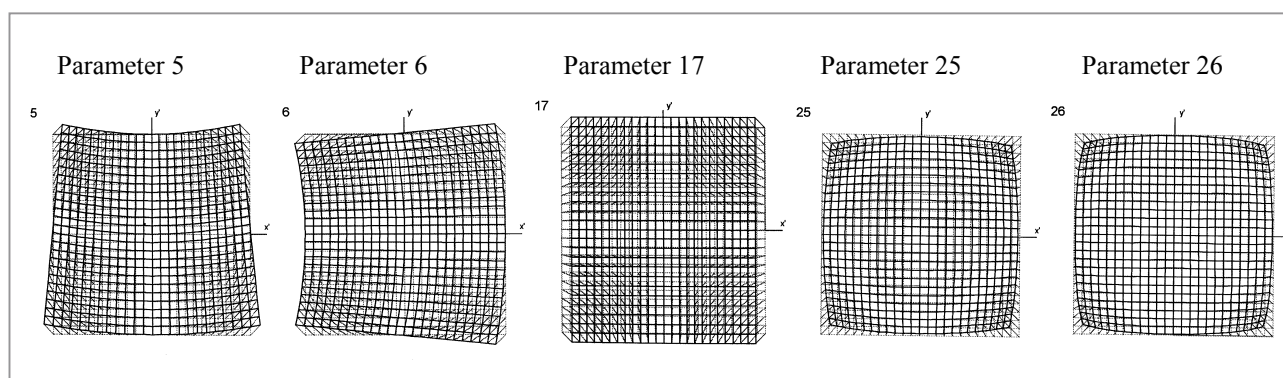


Figure 6: Additional parameters

We noticed radial and non-radial distortions. Softplotter, the software package we use for the DSM generation, only provides the possibility to correct the image for radial lens distortions. We developed a program to correct the images for the additional parameters. Besides, this program creates fiducials in the corners of the image. This simplifies the interior orientation in Softplotter.

Table 1 lists the estimated camera calibration parameters and their standard deviations for one of the three cameras. Similar results were obtained for the other cameras. Four calibrations were carried out with an average time interval of one month between the different epochs. The average value for each parameter is calculated out of four epochs. The difference of each epoch with the average is listed. The numbers in the table show that this difference is not larger than about three times the average standard deviation of the corresponding parameter. This demonstrates the stability of the system.

Camera 1	Average value	Average	epoch 1	epoch 2	epoch 3	epoch 4
Focal length ( $\mu\text{m}$ )	6034.3	2.1	1.5	-1.9	-6.3	6.7
Principal point X ( $\mu\text{m}$ )	-11.7	0.8	-2.2	0.5	-0.6	2.4
Principal point Y ( $\mu\text{m}$ )	69.6	0.9	1.6	1.9	-1.6	-1.7
Parameter 5	6.2	0.1	0.1	-0.3	-0.1	0.2
Parameter 6	1.6	0.1	0.1	-0.2	-0.3	0.3
Parameter 17	8.4	0.0	-0.1	0.2	0.0	-0.1
Parameter 25	111.5	0.5	-0.4	-0.5	0.4	0.4
Parameter 26	-12.2	0.9	-0.8	2.2	-1.5	0.3

Table 1: Results of camera calibration for camera 1

## 4 DIGITAL SURFACE MODEL GENERATION

### 4.1 The software for DSM generation

Softplotter, the program we used for the DSM generation, was developed for the use with aerial photographs. It provides accurate and efficient extraction of terrain and feature data from digital imagery. In the first step of the DSM generation process the camera data is defined. We used the exterior orientations that are produced by the calibration process. The images are corrected for the lens distortions beforehand. This makes that only the focal length and the coordinates of the fiducial marks had to be supplied. This information is different for each of the three cameras. The coordinates of the artificial fiducials define the location of the principal point. An interior orientation had to be carried out. No additional measurements in the images were necessary, because we used the exterior orientation results from the calibration.

A stereopair is created by resampling and rectifying the triangulated images into epipolar geometry such that the y-parallax is removed and the x-parallax is interpreted as differences in elevation. The so-called surface tool is used to create a Triangulated Irregular Network (TIN). This TIN collection is based on a least squares algorithm, which establishes correspondences by minimizing the sum of the squared differences between the grey levels in patches of the images. The strategy parameters are critical in producing a reliable TIN and affect the speed at which automatic correlation is completed (Gooch, 1998). The autocorrelation procedure incorporates a hierarchical approach in which correlations are performed at increasingly higher resolutions in the image pyramid. Interpolated points are ignored in the creation process. Softplotter returns an indication of the accuracy of the created DSM.

### 4.2 Combining the three surface models

We combined the three models of the three possible combinations of two cameras to increase the reliability of the created surface models. This is the advantage of using three cameras instead of the minimum of two cameras. With only two cameras there is no check on the generated DSM.

Softplotter offers the possibility to compare two different DSMs. This creates the opportunity to assess the achieved precision. The DSM that is generated in Softplotter is a TIN. In order to be able to combine the three models, the points have to be known in a regular grid. In Matlab, a software package specially designed for scientific and engineering numerical computation, the points are interpolated to the same regular grid using bicubic interpolation. The sampling interval is set to half the size of the grid size of the original TIN.

The three models are combined as follows. First the three TINs are interpolated to the same regular grid. Now we have three heights for every point. The average height of two models is compared with the height of the third model. If the difference is larger than twice the standard deviation computed from the differences between the two models, the value of the third model is removed and a new DSM value is calculated. The resulting DSM is the average of the three resulting models after removal of outliers. Optionally a 3 x 3 averaging filter is used to smooth the resulting DSM. This final DSM can be used to calculate the wound features of interest, such as the volume, surface and contour.

### 4.3 Determination of the volume

In order to determine the volume of a wound two surfaces have to be known: the measured surface of the wound and the original, healthy skin surface. The volume of the wound is sandwiched between those two surfaces. The original healthy skin has to be reconstructed from undamaged parts of the skin surrounding the wound. As a first step, the outline of the wound has to be defined. The second step is the reconstruction process itself. An interpolation method, such as cubic splines, has to be used to interpolate the original healthy skin (de Jong, 1997). As a final step, the area, volume, circumference and depth of the wound can be calculated from a three-dimensional grid created by the process described above. It has to be stressed that the majority of the errors in the reconstruction of the healthy skin will be eliminated in the difference between two volumes. These volume changes are used for assessing the healing process. Neglecting the effects of errors in the reconstruction of the healthy skin, the precision of the volume depends on the precision of the generated DSM and the depth of the wound. The precision of the volume can be approximated with:

$$\sigma_{vol} = vol \cdot \frac{\sigma_{depth}}{depth} = surf \cdot \sigma_{depth}$$

When the accuracy of the determined heights is 0.5 mm, and the wound has a depth of 5 cm, the accuracy of the volume equals 1% of the total volume.

## 4.4 Experiments

Different experiments were performed to review the achievable accuracy of the three-camera system. The first experiment consisted of a flat surface with texture. From this flat surface a DSM was generated. DSMs were also generated from plastic models of different sizes of pressure sores. These plastic models lack texture. We found that the lack of texture caused difficulties during the DSM matching process. Texture projection was added in the final experiments to review the improvements in the accuracy. The plastic wounds were also imaged again with texture projection. It turned out that the accuracy improved with the use of texture projection.

Figure 7 shows the created DSM for wound number 1. The figure shows that blunders are filtered out and that the resulting DSM is a smooth surface. Softplotter gives an indication of the theoretical precision of the generated DSM. The theoretical precision of the generated DSMs is at least 0.5 pixel. This corresponds, with a pixelsize of 0.0074 mm and an average distance of 30 cm, with a precision of 0.2 mm in object space.

This result seems to be too optimistic for the precision of the generated DSMs. The different models of the same objects are compared to get more insight in the achieved precision of the DSM. Numerical results of the experiments are summarized in table 2. The average, standard deviation and maximum value of the differences between the three models is indicated for all test objects, with and without texture projection. In most cases we found a normal distribution for the differences between two models.

Object (in mm)	Difference model 1/2 – 2/3			Difference model 1/3 – 2/3			Difference model 1/2 – 1/3		
	Avg.	Stdv.	Max.	Avg.	Stdv.	Max.	Avg.	Stdv.	Max.
Flat surface (texture)	0.329	0.398	1.324	0.230	0.456	2.320	0.336	0.578	2.428
Plastic wound 1 (no texture)	0.105	0.942	10.050	0.238	0.891	12.034	-0.121	0.990	16.579
Plastic wound 2 (no texture)	0.130	1.178	19.332	0.220	1.055	11.175	-0.326	1.307	11.468
Plastic wound 3 (no texture)	0.194	1.163	14.377	0.231	0.985	8.397	-0.195	1.249	7.614
Head wound (no texture)	0.049	1.188	8.405	0.078	1.018	8.814	0.030	0.971	11.220
Pressure sore (no texture)	0.240	1.499	7.048	-0.081	1.535	11.643	0.488	2.742	14.095
Pressure sore (texture)	0.279	0.753	4.210	0.327	0.676	5.174	-0.080	0.803	8.421

Table 2: Accuracy of created DSMs

The table shows that the repeatability that can be achieved for a flat surface with texture projection is about 0.5 mm in height. The repeatability that can be achieved for the plastic models of pressure sores, without texture projection, is better than 1 mm in height. Texture projection should improve the results. The precision that can be achieved for a pressure sore with texture projection is 0.7 mm in height.

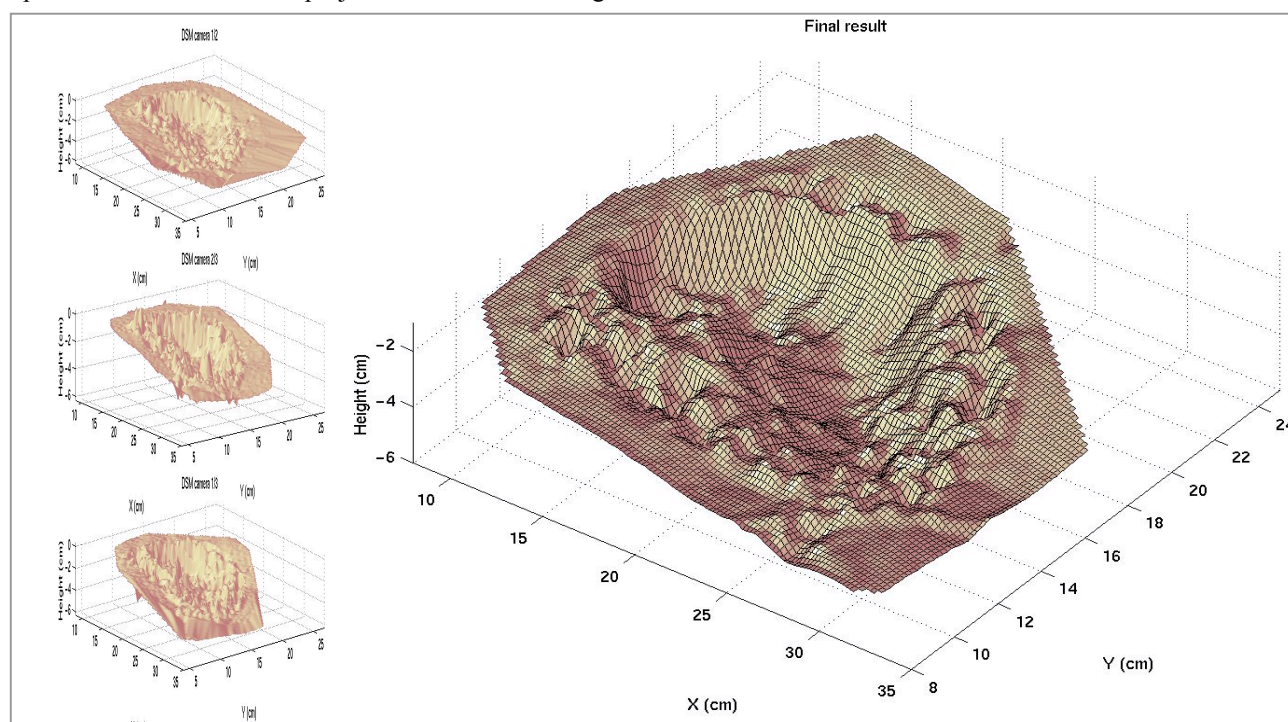


Figure 7: DSM of plastic wound 1

## 5 WOUND MEASUREMENT: THE FIRST RESULTS

Experiments with patients were carried out to measure wounds of humans. Different types of wounds, not only pressure sores, were recorded. The measurement process lasts in total only 5 minutes per patient. The calibration has to take place once for each recording session because the cameras and the system are fairly stable (section 3.3). Differences only occur after transportation of the system.

We found that wounds with a moist and a flat surface are hard to record, because of the many occurring reflections. We were unable to measure wounds with a very steep surface completely, because the wound is only partly visible in some images. In the plastic models we saw that lack of texture makes the matching process difficult. This was also true for real wounds. Therefore, we added texture projection in the second image acquisition session with patients.

Table 2 lists the results of three patients that gave fairly good results. The first patient had a large wound on her head. This wound showed enough texture to give a fairly good matching result. The second patient had a pressure sore on the buttock. The skin caused too many reflections and lacked texture. The third patient also had a pressure sore on the buttock. This time texture projection was used, which resulted in a much smoother surface model. Figure 8 shows the images taken with the three different cameras and the final result of the third patient.

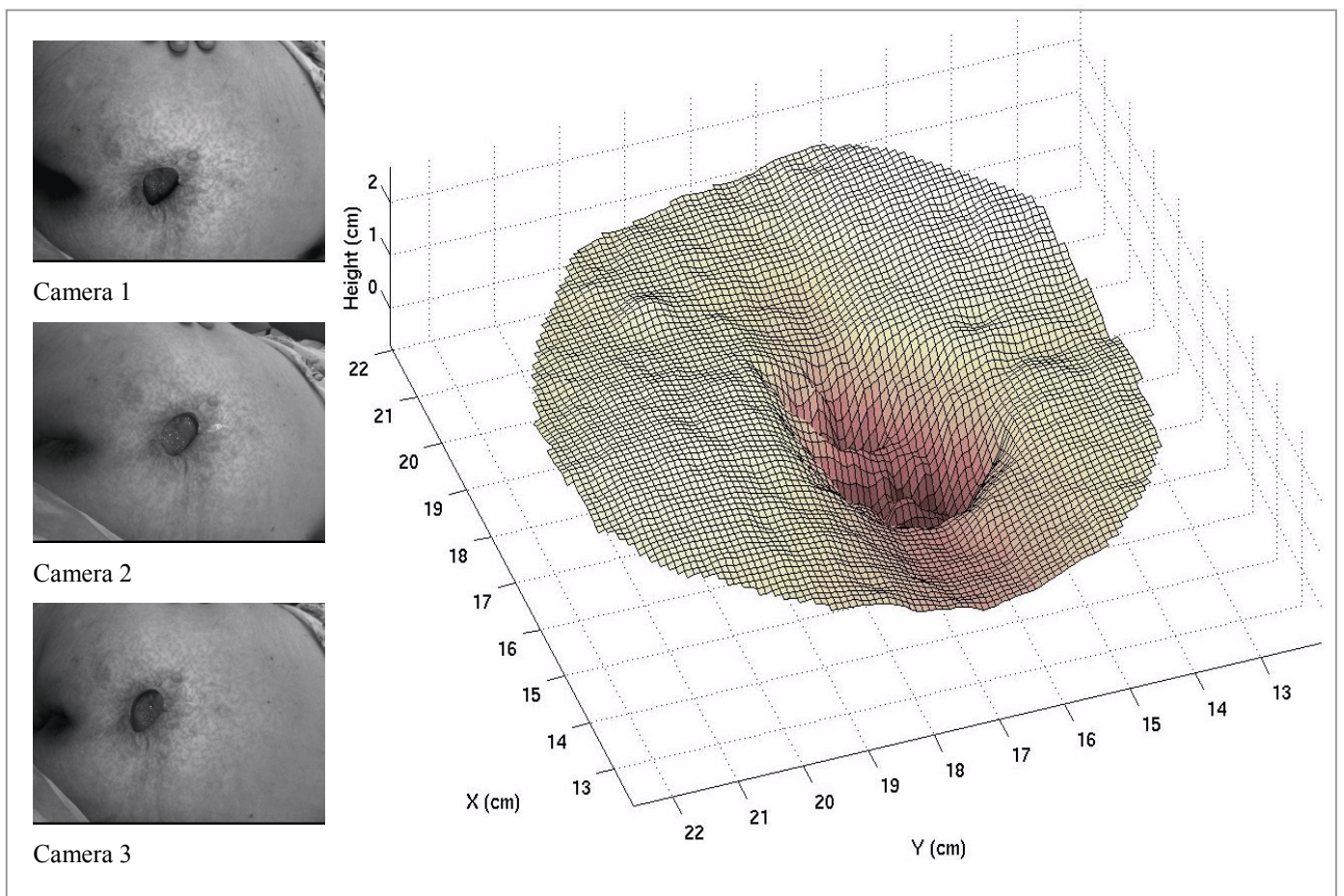


Figure 8: Created DSM of head wound

## 6 CONCLUSIONS AND FUTURE RESEARCH

This research provided that digital close-range photogrammetry is an accurate, efficient, fast and non-contact method to measure features of pressure sores in a very patient-friendly way. With the use of texture projection a DSM of a flat surface can be generated with a precision of 0.4 mm in height. With texture projection the precision of the DSM of a pressure sore can be better than 0.7 mm in height. The reliability is improved by combining the three different models into one final DSM.

Future work has to concentrate on the integration of the components in one user-friendly real-time measurement system, and on further improvement of the accuracy of the system.

The precision of this system could be improved by a higher camera resolution. The cameras used in this research have a relatively low (standard video) resolution. The precision and the reliability may be improved by adding more cameras to the system. However, this has the disadvantage of a larger and thus less flexible system. Adding more cameras has the advantage that different non-correlated models can be compared and combined into one final model. More research has to be performed on the use of texture projection. Adding texture projection improves the matching process and thereby the accuracy of the resulting DSM. Experiments with different types of texture projection could be carried out.

## ACKNOWLEDGEMENTS

The authors would like to thank the 'Centre for Human Drug Research' in Leiden, The Netherlands, that provided the video cameras and 'Het Groene Hart Ziekenhuis' in Gouda, The Netherlands, for letting us work with their patients. Finally we would like to thank the patients who were willing to participate in the experiments.

## REFERENCES

- Bulstrode, C.J.K., A.W. Goode, P.J. Scott, 1986, Stereophotogrammetry for measuring rates of coetaneous healing: a comparison with conventional techniques, *Clinical Science*, 71 (4): p. 437- 443.
- Eriksson, G., A.E. Eklund, K.Torlegard en E. Dauphin, 1979, Evaluation of leg ulcer treatment with stereophotogrammetry, *British Journal of Dermatology*, Vol. 101, p. 123-131.
- Gooch, M. J. and J. H. Chandler, 1998, Optimization of strategy parameters used in automated Digital Elevation Model generation, *IAPRS*, 32(2), p. 88-95.
- Health Council of the Netherlands: Pressure Ulcers, 1999, Health Council of the Netherlands: publication no. 1999/23, The Hague, The Netherlands (in Dutch).
- de Jong, L., 1997, Medische fotogrammetrie; Digitale close-range fotogrammetrie voor het meten van doorligwonden, Msc thesis, TU-Delft, Afdeling Geodesie, Delft, The Netherlands (in Dutch).
- Kruck, E., 1998, BINGO-F, Bundle Adjustment for Engineering Applications, Version 4.0, Gesellschaft für Industriephotogrammetrie, Aalen.
- Ng, K.C., B.F. Alexander. S.H. Boey, S. Daly, J.C. Kent, D.Q. Huynh, R.A. Owens, P.E. Hartmann, 1994, Biostereometrics – a non-contact, non-invasive shape measurement technique for bioengineering applications, *Journal of the Australian Physical & Engineering Sciences in Medicine*, September 1994, vol. 17, no. 3, p. 124-130
- Plassman, P., B.F. Jones, E.F.J. Ring, 1995, A structured light system for measuring wounds, *Photogrammetric Record*, Vol. 15, No. 86, p. 197-203.
- Resch, C.S., E. Kerner, C. Martin, J.P. Heggens, M. Scherer, J.A. Boertman, R. Schileru, 1988, Pressure sore volume measurement. A technique to document and record woundhealing", *Journal of the American Geriatrics Society*, vol. 36, no. 6, p 675-678.
- Softplotter, 1999, Softplotter User Manual 2.0, Autometric Inc., Bangor, U.S.A.
- Wester-Ebbinghaus, W., 1983, Einzelstandpunkt-Selbstkalibrierung – ein Beitrag zur Feldkalibrierung von Aufnahmekammern, *Deutsche Geodeatische Kommission Reihe C*, Heft Nr. 289.

[Http://members.xoom.com/hvdijk](http://members.xoom.com/hvdijk), last modified February 19<sup>th</sup>2000.